RADIOMETRIC CHARACTERISATION OF A VNIR HYPERSPECTRAL IMAGING SYSTEM FOR ACCURATE ATMOSPHERIC CORRECTION

Lucas Martínez, Fernando Pérez, Roman Arbiol, Anna Tardà

Institut Cartogràfic de Catalunya (ICC). Parc de Montjuïc s/n, 08038. Barcelona, Spain.
Lucas.Martinez@icc.cat

ABSTRACT

The Institut Cartogàfic de Catalunya (ICC) regularly operates a Compact Airborne Spectral Imager (CASI) sensor. For this system an atmospheric correction algorithm was developed to simultaneously correct multiple overlapping images taken from different heights. First, the algorithm estimates the main atmospheric parameters with an inversion procedure using either radiometric ground measurements or image homologous areas plus a single ground measurement. Then, the code is applied to the images to obtain atmospherically corrected hyperspectral imagery. The algorithm was applied in the frame of ICC-Banyoles 2005 experiment (Spain) using multi-height imagery and field simultaneous reflectance measurements. In the validation step, the standard deviations obtained with both inversion methods were similar. In order to improve these results, the smiling effect (spectral shift) for the sensor is characterized by locating O_2 absorption bands in the NIR for each CASI look direction. Additionally, a more accurate spectral sensitivity for each band has been calculated. These improvements are applied to EuroSDR-Banyoles 2008 experiment's (Spain) imagery. These results show a substantial improvement on the atmospheric correction at the absorption regions when compared to field reflectance measurements. This behaviour advises the inclusion of these developments in the inversion system.

***Index Terms*—**CASI, atmosphere, inversion, smile, spectral sensitivity.

1. INTRODUCTION

Hyperspectral remote sensing data are a common tool for applications such as agriculture, forestry, water quality, environment, etc. The acquisition of these data at high spatial resolution has been possible for many years by means of airborne sensors and more recently from satellites. The ICC-CASI configuration is a CASI 550 system synchronized with an Inertial Navigation System (INS) and a Differential Global Positioning System (DGPS). The integrated system is designed to convert the sensor imagery captured by the CASI into high quality orthoimages, useful for cartographic purposes [6].

The radiometric quality of the remote sensing data is essential to obtain reliable results. Radiance measured by a sensor depends on the illumination geometry and on the reflectance characteristics of the observed surface. However, several atmospheric processes disturb this measurement: gas absorption and both Rayleigh and Mie scattering [3].

The best results in atmospheric correction are obtained through a radiative transfer approximation. However, radiative transfer approaches need an accurate prior estimation of different atmospheric constituents such as water vapour, aerosols and ozone concentration. Aerosols and water vapour concentrations are extremely space and time-dependent. While simultaneous field measurements can be used in an inversion of the radiative transfer code in order to obtain the optimal atmospheric parameters, an alternative solution is presented in this communication. It relies on the fact that in a multi-height and overlapping set of images over the same area small homogeneous targets are captured from different angles and heights. These areas can also contribute to atmospheric parameters estimation in the inversion of the radiative transfer code. Then, these parameters can be used to perform the atmospheric correction of the whole set of images by using a radiative transfer code.

The smoothness of the recovered spectra depends on the accuracy of the sensor radiometric characterisation. The ICC-CASI system is periodically maintained and re-calibrated at laboratory by the manufacturer and a calibration report is delivered. The calibration report does not include accurate information about the smiling effect (spectral shift in the relationship between bands and wavelengths when measured at different CCD columns) or the detailed spectral sensitivity of the 288 individual bands of CASI VNIR sensor. To overcome this difficulty, the spectral calibration provided by the manufacturer is enhanced with a method to match the O_2 absorption region (765nm) in the NIR for all the system look directions. Moreover, the nominal spectral resolution (FWHM) reported at the CASI 550 Product Brochure of 2.2nm is an optimistic estimation for central wavelengths. Real bandwidth of the individual channels increases up to 8nm, as reported by the manufacturer. Hence a modelization of the spectral response of the individual CASI bands is proposed to avoid miss- and over-corrections in the atmospheric correction system.

In the following sections we make a description of the proposed algorithms and present the results obtained from its application to a dataset acquired over Banyoles (Spain) in two campaigns: ICC-Banyoles 2005 [5] and EuroSDR-Banyoles 2008 [1]. In situ reflectance measurements, taken almost simultaneously to CASI flights, have been used to test these methodologies, validate the atmospherically corrected reflectances, and assess the impact of an accurate radiometric characterisation on the atmospheric correction.

2. METHODOLOGY

2.1. Manufacturer radiometric sensor calibration

The CASI 550 standard manufacturer sensor calibration procedure includes the so-called g-coefficients and a measure of the spatial and spectral spectrograph alignment. The g-coefficients are polynomial coefficients that relate the sensor CCD lines to the band central wavelength for all the look directions. The spectrograph alignment is a check to verify that the sensor complies with its calibration specifications. Neither the spectral sensitivity of the 288 bands nor the dependencies of the g-coefficients with the look direction are provided.

2.2. Inversion procedure

The objective is to retrieve the atmospheric optical parameters - Aerosol Optical Thickness (AOT) and water vapour content- for the whole area where the atmospheric correction is performed. For these estimations, the atmospheric state is considered invariant within the area covered by the image.

Two methodologies are proposed for parameter estimation [4]. First, in an approach similar to that of Guanter et al. [2], the inversion procedure is performed by minimizing a cost function δ_{mes}^2 that measures the difference between atmospherically corrected reflectances and field measurements

$$\delta_{mes}^2 = \sum_{j}^{images} \sum_{m}^{measurements} \sum_{\lambda_i}^{wavelenght} \frac{1}{\lambda_i^2} \left(\rho_{j,m,\lambda_i}^{corrected} - \rho_{j,m,\lambda_i}^{field} \right)^2 \qquad (1),$$

where ρ_{field} is the spectral reflectance measured on the field, $\rho_{corrected}$ is the atmospherically corrected spectral reflectance calculated with the radiative transfer code and λ_i is the equivalent wavelength for each sensor band. In a second approach, the inversion procedure is performed by minimizing a more complex cost function δ_{hom}^2 that consists of the difference between atmospherically corrected reflectances calculated on homologous areas observed on different images, plus one field measurement.

$$\delta_{hom}^2 = \sum_{j,k}^{images} \sum_{h}^{homo} \sum_{\lambda_i}^{wavelenght} \frac{1}{\lambda_i^2} \left(\rho_{j,h,\lambda_i}^{corrected} - \rho_{k,h,\lambda_i}^{corrected} \right)^2 + \delta_{1\text{-}mes}^2 \qquad (2).$$

Both cost functions are weighted by λ_i, to take into account the strong wavelength dependency of the atmospheric effects and increase the significance of low wavelength values.

The 6S radiative transfer code [8] was selected to calculate the atmospherically corrected reflectances. The standard continental model was selected to represent the aerosol types and the standard US62 atmosphere pressure and temperature profiles were selected as inputs for the code. Total water vapour amount and AOT were set as the parameters to be calculated.

2.3. Atmospheric correction

Taking into account the interaction phenomena described in Staenz and Williams [7], it is possible to express the radiance at the sensor, when observing a horizontal surface, as

$$L^* = A \frac{\rho_c}{\left(1 - \langle \rho_e \rangle S\right)} + B \frac{\langle \rho_e \rangle}{\left(1 - \langle \rho_e \rangle S\right)} + L_a \qquad (3),$$

where ρ_c is the corrected reflectance of the surface, $<\rho_e>$ is the corrected reflectance of the neighbourhood, S is the atmospheric albedo, L_a is the radiance backscattered to the sensor and A , B are coefficients related to the direct and diffuse radiance.

Therefore, the corrected reflectance ρ_c- or BOA reflectance- for the observed surface is

$$\rho_c = \frac{\left(L^* - L_a\right)\left(1 - \langle \rho_e \rangle S\right) - \langle \rho_e \rangle B}{A} \qquad (4).$$

The parameters A, B, S and L_a characterize both observation and illumination geometries and the atmospheric conditions. Their values do not depend on the observed surface reflectance, or the neighbourhood's. They are calculated from the magnitudes L_g, which is the radiance entering the sensor from the observed surface, and $L_{p,}$ the radiance entering the sensor from the neighbourhood of the observed surface and backscattered by the atmosphere towards the sensor.

$$L_g = A \frac{\rho_c}{1 - S\rho_c} \qquad L_p = B \frac{\rho_c}{1 - S\rho_c} + L_a \qquad (5).$$

Both L_g and L_p can be obtained by means of radiative transfer codes working in direct form. The values of A, B, S and L_a are directly obtained by solving the corresponding equation systems. The radiative transfer simulations are performed using the synchronous atmospheric data obtained in the inversion procedures and stored in a Look-Up Table system. Then, atmospheric correction is possible on the images by using equation 4.

The neighbourhood's corrected reflectance $<\rho_e>$ is obtained during the atmospheric correction entering the whole neighbourhood in equation 4 as if it were a hypothetic single pixel located in a uniform reflectance environment. So, in that expression $<\rho_e>$ will be equal to ρ_c. Also, its radiometry L* is calculated using the whole neighbourhood pixels radiometry. From these hypotheses, the value of $<\rho_e>$ will be

$$< \rho_e >= \frac{L^* - L_a}{A + B + S\left(L^* - L_a\right)} \qquad (6).$$

2.4. Spectral shift characterization

Spectral shift characterization is based on the hypothesis of global g-coefficients that need to be identically shifted for all the wavelengths for each look direction. The proposed methodology exploits the presence of the O_2 atmospheric absorption band (765nm) over a high reflectance cover in that wavelength. To determine the spectral shift a non-ortorectified hyperspectral image over a vegetated area is aggregated in the along-track direction. This process generates a one-line image with 550 across-track spectral samples (look directions). Then, a subpixel Pearson correlation is computed for each one of the 550 spectra with a vegetation spectrum processed with the 6S code [8] to take into account the effect of the O_2 absorption band. The estimated spectral shift is then applied to the original image and the

radiometric bands are spectrally resampled to fit the CASI channel nominal limits described by the g-coefficients.

2.5. Spectral sensitivity characterization

The first approximation to the sensitivity of the bands was a rectangular response between the limits of each channel. This simple estimation works fine to correct from atmospheric scattering but proves insufficient to solve the absorption regions. The manufacturer was then asked about the sensitivity of the bands and we received a polynomial relationship between FWHM and wavelength that shows values up to 4 times the nominal FWHM of the sensor (Figure 1).

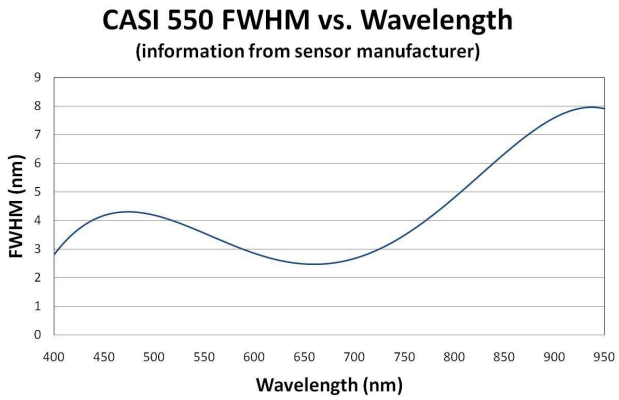

Figure 1 CASI 550 relationship between FWHM and wavelength provided by the manufacturer.

To take into account this effect, a Gaussian response for each individual CASI band is considered. When the sensor is configured to add bands, individual responses are also added to generate the spectral response.

3. DATASET

3.1. ICC Banyoles 2005 experiment

On June 29th CASI images were acquired between 10-11am on Banyoles (Spain) radiometric test field. Simultaneously, a field campaign was developed to perform field reflectance measurements using an ASD FieldSpec Pro radiometer [5]. For the second inversion methodology, 23 areas with adequate spatial homogeneity and spectral reflectance range were manually selected. As a field measurement, a bare soil ground target was used

3.2. EuroSDR Banyoles 2008 experiment

On July 15th CASI images were acquired between 9-11am on the same Banyoles radiometric test field. Simultaneously, a field campaign was developed to perform the reflectance measurements using GER 3700 and UNISPEC UNI003 radiometers [1].

4. RESULTS

The minimization of the cost functions in (1) and (2) was performed by a Simplex method, with climatological data for the initialization of the algorithm. Table 3 shows the total water vapour contents and the climatological visibilities from 6S code, related to AOT for ICC Banyoles 2005 experiment CASI imagery.

Inversion data source	Water vapour (g/cm2)	Visibility (km)
Field measurements	2.50	8.4
Homologous areas & 1 field measurement	2.42	12.4

Table 3 Inversion parameters obtained (Banyoles2005 data).

The atmospheric parameters were then used to perform the atmospheric correction of the whole set of Banyoles 2005 images. After that, the corrected images were compared with field reflectance measurements to assess the accuracy of the procedure. Table 4 shows the results of the validation for both methodologies in terms of global shift and σ^2 for all the images.

Inversion data source	Reflectivity shift	Reflectivity σ^2
Field measurements	0.000	0.008
Homologous areas + 1 field measurement	0.001	0.008

Table 4 Validation of atmospheric correction (Banyoles2005 data).

Figure 2 shows the results of the smiling effect calculation on EuroSDR Banyoles 2008 CASI imagery. The range of the spectral shift is 2.75nm and the maximum absolute value is 1.5nm. These results have the same order of magnitude as the spectral width sampling of the sensor: 1.9nm. So, the spectral shift of the CASI 550 sensor is not negligible if accurate radiometric results are desired.

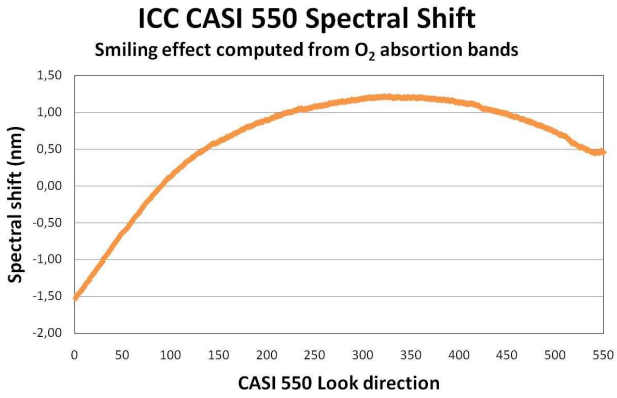

Figure 2 ICC CASI 550 Spectral Shift (Smiling effect) in nm computed by Pearson correlation of O_2 absorption bands (765nm) with absorption profiles modelled with 6S radiative transfer code.

The atmospheric correction system, when applied to a CASI image from Banyoles 2008, yields the spectra shown in Figure 3. On the other hand, when the software is modified to take into account the spectral sensitivity of the CASI bands and the correction is applied to the same image, previously corrected from smile effect, the results shown in Figure 4 are obtained. In both cases the atmospheric parameters used in the radiative transfer calculation are just climatological standard atmospheric parameters (and then not derived from any inversion procedure).

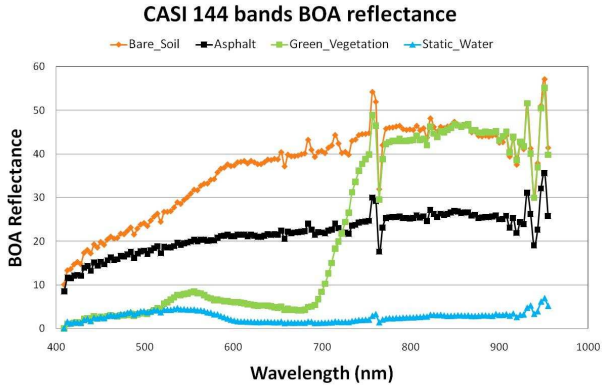

Figure 3 Banyoles 2008 atmospherically corrected CASI image without smiling and with nominal spectral sensitivity.

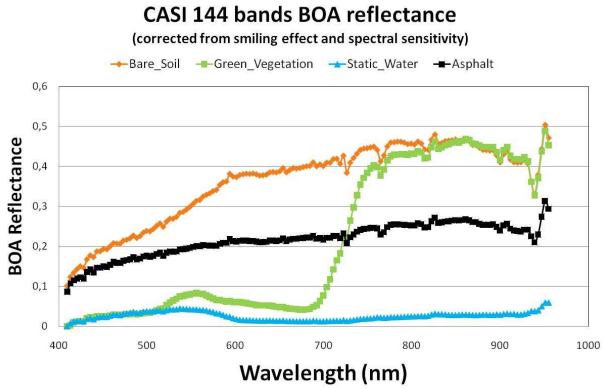

Figure 4 Banyoles 2008 atmospherically corrected (standard atmospheric parameters) CASI image with smiling and proposed spectral sensitivity.

The results indicate that, when smiling effect and spectral sensitivity are taken into account, the atmospheric correction yields fewer artifacts on the atmospherically corrected spectra, even when only standard atmospheric parameters are used. The small artifacts still remaining around the absorption bands could be explained by a frequency dependence of the smiling effect, signal-to-noise ratio too week, etc. This point is currently being investigated.

5. CONCLUSIONS

Two methodologies for retrieval of atmospheric parameters by means of an inversion procedure have been compared. Compatible atmospheric parameters are obtained in the inversion process using both methodologies. In the validation step, similar standard deviations are also obtained in both cases. We can then conclude that an inversion procedure using homologous areas plus a single field measurement yields accurate atmospheric parameters with less ground information. Non-negligible values for the spectral shift are obtained for the CASI 550 sensor. Moreover, when smiling effect and spectral sensitivity are taken into account, the atmospheric correction yields fewer artefacts on the spectra. This behaviour advises the inclusion of these developments in the inversion system.

ACKNOWLEDGMENTS

The authors are very grateful to Centre de Recerca Ecològica i Aplicacions Forestals, Instituto de Desarrollo Regional UCLM and Centro de Estudios y Experimentación de Obras Públicas for their collaboration in Banyoles 2005 and 2008 experiments.

REFERENCES

[1] Arbiol R. and Martinez L. “ICC-Banyoles 2008 Campaign in the framework of EUROSDR Radiometry Project. Project description and preliminary results,” *International Geomatic Week*, Barcelona 3 - 5 March 2009.

[2] Guanter, L., Alonso, L., Moreno, J. “A method for the surface reflectance retrieval from PROBA/CHRIS data over land: Application to ESA SPARC campaigns”. *IEEE Transactions on Geoscience and Remote Sensing*, 43, 2908-2917, 2005.

[3] Kaufman, Y. J. “The atmospheric effect on remote sensing and its correction”. In Asrar, G., editor, *Theory and Applications of optical Remote Sensing*, Wiley and Sons, New York, 1989.

[4] Martínez L., Palà V., Arbiol R, Pérez F. and Tardà A. “Atmospheric correction algorithm applied to CASI multi-height hyperspectral imagery”, *RAQRS II*. 25-29th September 2006 València.

[5] Martínez L. and Arbiol R. “ICC experiences on DMC radiometric calibration. International,” *Calibration and Orientation Workshop EuroCOW 2008*. Castelldefels, 30th genuary – 1st February 2008.

[6] Palà, V., Alamús, R., Pérez, F., Arbiol, R., Talaya, J.”El sistema CASI-ICC: un sensor multiespectral aerotransportado con capacidades cartográficas,” *Revista de Teledetección*. 12, p. 89-92, 1999.

[7] Staenz, K., and Williams, D.J., “Retrieval of Surface Reflectance from Hiperespectral Data Using a Look-up Table Approach,” *Canadian Journal of Remote Sensing*, Vol 23, nº4, 354-368, 1997.

[8] Vermonte, E., Tanré, E.D., Deuzé, J.L., Herman M., and Morcrette, JJ “Second simulation of the satellite signal in the solar spectrum, 6S: an overview,” *IEEE Transactions on Geoscience and Remote Sensing*, 35, 675-686, 1997.